Multi-user indoor ultra-wideband wireless communication using polyphase spreading sequences

Ambroze, MA; Martin, PA; Tomlinson, M; Taylor, DP

Published in:
IET Communications

DOI:
10.1049/iet-com.2014.0131

Publication date:
2015

Multi-user Indoor UWB Wireless Communication using Polyphase Spreading Sequences

Marcel A. Ambroze†, Philippa A. Martin°, Martin Tomlinson†, Desmond P. Taylor°,

† School of Computing and Mathematics, University of Plymouth, Drake Circus, Plymouth, PL8AA, UK. {m.tomlinson,m.ambroze}@plymouth.ac.uk.

○ Department of Electrical and Computer Engineering, University of Canterbury, Private Bag 4800, Christchurch 8140, New Zealand. {philippa.martin,desmond.taylor}@canterbury.ac.nz.

Abstract

In this paper we design a multi-user ultra-wideband system for indoor wireless communication. The proposed system is useful in multipath radio reception as the full multipath diversity gain is achieved. The system has multiple transmitters and receivers. They use polyphase spreading waveforms which feature low levels of mutual interference and enable each of the channel impulse responses to be measured free from distortion continuously with each data symbol transmission. A key feature of the proposed system is that for the case of a single radio path the waveforms used for transmission produce outputs from the corresponding cross correlators in the receiver, which are zero on both sides of the main correlation peak. This lasts for a duration in excess of the expected delay spread of the radio channel. The effects of the low levels of mutual interference are reduced further by using time and frequency hopping, forward error correction and soft decision decoding.

I. Introduction

We consider an indoor *ultra-wideband (UWB)* wireless communication system with multiple transmitters and receivers. Any wireless frequency could be used, but the most likely applications

are in the unlicensed *industrial, scientific and medical (ISM)* and *short range devices (SRD)* frequency bands which feature a wide bandwidth. We consider short range, low power wireless links. When received within a building they feature high attenuation, shadowing, and multipath propagation with wide variations in signal strength. Within a building, the total delay spread of the multipath signals is typically 100 nsec, and individual paths are resolvable down to 5 psec [2], [3]. The proposed system continuously measures the propagation characteristics of the radio channel so as to maximize the multipath processing gain in a Rake receiver and is resistant to co-channel interference enabling several users to operate simultaneously in the same frequency band.

A UWB communications system that periodically transmits narrow pulses with the period chosen to exceed the delay spread of the multipath signals can use a Rake receiver to maximize the received power [5]. Effectively, the narrow pulses resemble impulses enabling the impulse response of the channel to be measured automatically with each transmission. Consequently the Rake receiver becomes the matched filter for the channel [1].

An inconvenience with the transmission of narrow pulses, as in the original UWB system [5], is that the transmitter has to transmit a high level of peak power relative to the average power. One answer is to use spreading sequences, such as the binary Barker sequences [8], to modulate each data bit and use a cross correlator in the receiver to produce an impulse like output. However, with Barker sequences the cross correlation function around the main peak output is not zero and so an inexact *channel impulse response (CIR)* is measured leading to performance degradation in the Rake receiver.

The key novelty of the proposed system is the specially designed polyphase spread spectrum sequences (patented by the authors [25]) that enable the receiver to measure the exact impulse response of the radio channel continuously. Due to the design of the sequences, the measurement of the impulse response is free from distortion, enabling a Rake processor to achieve full multipath processing gain and adapt to changing channel propagation. In addition, when multiple signals are transmitted using the same radio carrier frequency, the spread spectrum sequences are designed such that only relatively low levels of mutual interference are experienced in the cross correlators in the receivers. The approach is to modulate the carrier, for each user with a unique sequence of chosen phase shifts such that at the output of the corresponding cross correlators in the receiver, an impulse like output is produced with a zero response in the vicinity of the

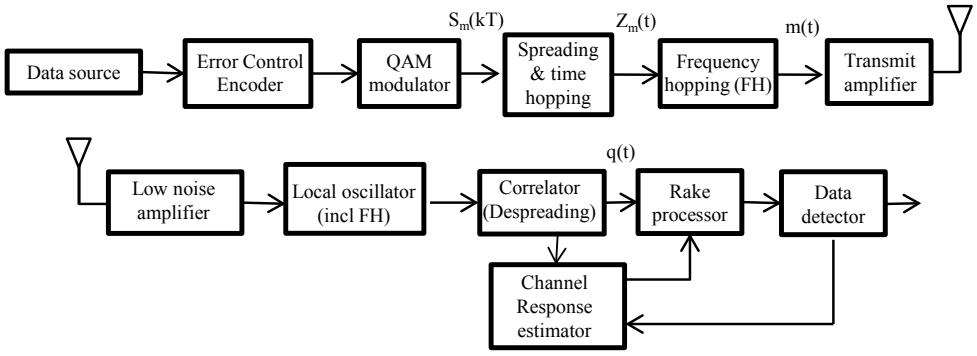

Fig. 1: Overall system featuring channel estimation and Rake processing.

main peak output. To mitigate any residual co-channel interference both time hopping and non coherent frequency hopping are used for each user.

The paper is organized as follows. The system model used is described in Section II, including the basic transmitter and receiver design. Then the design of the polyphase spreading sequences, CIR estimation and Rake processing are covered in Section III. An evaluation of the communications channel is included in Section IV. Simulation results are shown in Section V and finally conclusions are drawn in Section VI.

II. System Model

A block diagram of the proposed system model is shown in Fig. 1. Since an indoor UWB system is considered, a multipath log-normal channel model is used [26]. The attenuation (squared) of a path is given by the log-normal random variable

$$\alpha^2 = 10^{\sigma_a Y/10}, \tag{1}$$

where $\sigma_a = 5$ dB and Y is a Gaussian random variable, $\mathcal{N}(0,1)$ [2], [3]. The *probability density function (pdf)* of α^2 is

$$p_{\alpha^2}(y) = \frac{10}{\ln(10)\sqrt{2\pi}\sigma_a y} \int_0^\infty e^{-10\log_{10}(x)/2\sigma_a^2} dx. \tag{2}$$

A. Transmitter

We consider a system with M active users and describe the transmitter for user m. The data is first passed through an error correction encoder. Then the encoded data is mapped to a signal constellation. In general, the data symbols are mapped to a constellation with complex values, which are denoted using

$$S_m(kT) = s_{m,I}(kT) + j s_{m,Q}(kT), \tag{3}$$

where T is the symbol period and k is an integer. In the following we assume *quadrature amplitude modulation (QAM)*. Each data symbol is multiplied by a complex spreading sequence of length N_c chips, $X_m(nT_c)$ for $n = 0, \cdots, N_c - 1$, where $N_c T_c \leq T$. This results in the encoded complex spread spectrum sequence given by

$$S_m(kT) \sum_{n=0}^{N_c-1} X_m(nT_c)\delta(kT - nT_c), \tag{4}$$

where $\delta(t)$ is the standard Kronecker delta function, T_c is the chip period,

$$x_{m,I}(t) + j x_{m,Q}(t) = \sum_{n=0}^{N_c-1} X_m(nT_c)\delta(t - nT_c), \tag{5}$$

$x_{m,I}(t)$ and $x_{m,Q}(t)$ are the real and imaginary parts of (5), respectively.

Each user employs a different complex spreading sequence and cross correlation is used in the receiver to detect each user's signal and to minimize the effects of co-channel interference. Any peaks in the respective cross-correlation functions will result in peaks of co-channel interference levels and these are reduced in effect by employing time-hopping and discrete frequency hopping amongst the channels available. We use the frequency and time hopping generators of [22], which are based on pseudo-random generators designed to produce a uniform probability distribution and suitable CMOS implementations for UWB communications. For such hopping having a uniform probability distribution, the number of interferers in a given channel at a given time follows a binomial distribution. Each error control codeword spans N QAM symbols. This provides for further soft decision processing gain in the receiver.

The transmitted complex baseband signal for each codeword, prior to frequency hopping, can be written as

$$\mathcal{Z}_m(t) = \sum_{k=0}^{N-1} S_m(kT + t_h) \sum_{n=0}^{N_c-1} X_m(nT_c + t_h)\delta(t - nT_c - t_h). \tag{6}$$

The time hop value, t_h, is constant over a signal duration equal to the frequency hopping period, but varies pseudo randomly every frequency hop. We choose $T > N_c T_c$ to allow for time hopping with $X_m(t) = 0$ for $t_h - \frac{N_c T_c}{2} \geq t \geq t_h + \frac{N_c T_c}{2}$. Here, the symbol period is chosen to be $T = 2N_c T_c$ such that $-\frac{N_c T_c}{2} \leq t_h \leq \frac{N_c T_c}{2}$.

If we directly implemented the transmitted signal as in (6), we would require four *finite impulse response (FIR)* filters. However, instead we can phase shift by $\frac{\pi}{4}$, inputting the sum and difference of the real and imaginary components of $\mathcal{Z}_m$ into two FIR filters, respectively. Each tap in the FIR filter is separated from the next by a delay equal to the chip period T_c [1] and has impulse response given by (5).

The centre carrier frequency f_c is frequency hopped an integral number of times for each codeword. Typically the system is arranged to have 5 to 10 frequency hops per codeword. The modulated signal can then be written as

$$m(t) = \quad Re\left\{\sum_{k=0}^{N-1} S_m(kT + t_h) \sum_{n=0}^{N_c-1} X_m(nT_c + t_h)\ \delta(t - nT_c - t_h) \times e^{(j2\pi f_c t)}\right\}. \qquad (7)$$

This form of UWB is impulse radio equivalent. The proposed spreading sequences will produce the same results after correlation in the receiver as transmitting impulses, but without peak power implications.

B. Receiver Matched Filtering and CIR Estimation

The received signal is down converted to quadrature baseband components using a local oscillator with frequency reference $cos(2\pi f_c t + \phi)$, which corresponds to the frequency hopped transmitter plus an arbitrary phase shift ϕ.

For each user, the receiver carries out despreading of the polyphase sequences by using waveform-matched FIR filters. This is followed by CIR estimation. The despreading filter for user u which matches the spreading sequence of the transmitter $x_{u,Q}(t)$ is given by

$$\hat{x}_{u,Q}(t) = -Im\left\{\sum_{n=0}^{N_c-1} X_u((N_c - 1 - n)T_c)\delta(t - nT_c)\right\}. \qquad (8)$$

It should be noted that the coefficients of $x_{u,Q}(t)$ and $\hat{x}_{u,Q}(t)$ are the same, but of opposite sign as these are the phase quadrature component corresponding to the imaginary component, and are in reverse order. The filter to the in-phase component $x_{u,I}(t)$ is denoted $\hat{x}_{u,I}(t)$ and is given

by

$$\hat{x}_{u,I}(t) = Re\left\{\sum_{n=0}^{N_c-1} X_u((N_c-1-n)T_c)\delta(t-nT_c)\right\}. \tag{9}$$

The complete expression for the result of the signal processing in the receiver of the sum of all transmitted signals plus noise is complicated and tends to obscure the different operations within the receiver. For clarity the analysis used below is piecemeal and for convenience we use the pre-envelope complex model of [1], [9]. The correlator shown in Fig. 1 is implemented using FIR matched filters. For the receiver selecting user u, its output is complex and can be represented, ignoring the effects of noise, as

$$\begin{aligned} q_u(t) = &\sum_{m=0}^{M-1}(s_{m,I}(t-n\tau) + js_{m,Q}(t-n\tau)) \otimes (x_{m,I}(t) + jx_{m,Q}(t)) \otimes c_{u,m}(t-\tau_m) \\ &\otimes e^{j\phi_{u,m}(t)}(\hat{x}_{u,I}(t) - j\hat{x}_{u,Q}(t)), \end{aligned} \tag{10}$$

where $\otimes$ represents the standard convolution integral [1]. The CIR as seen at the receiver for user u as a result of the transmission from user m is denoted by $c_{u,m}(t-\tau_m)$ and $\phi_{u,m}(t)$ is the received phase shift of this signal. There are M users and M received signals at the receiver for user u.

The autocorrelation function of the spreading sequence employed by user u is given by

$$\mathcal{A}_u(t) = \int_0^{N_cT_c} (x_{u,I}(\tau) + jx_{u,Q}(\tau))(\hat{x}_{u,I}(\tau+t) - j\hat{x}_{u,Q}(\tau+t))d\tau. \tag{11}$$

The cross correlation function of the spreading sequence employed by user u against that for user m is given by

$$\Upsilon_{u,m}(t) = \int_0^{N_cT_c} (x_{m,I}(\tau) + jx_{m,Q}(\tau))(\hat{x}_{u,I}(\tau+t) - j\hat{x}_{u,Q}(\tau+t))d\tau. \tag{12}$$

As convolution can be carried out in any order, the output of the correlator of Fig. 1, $q_u(t)$ from (10) simplifies to an expression for the wanted signal plus an expression for the co-channel interference, given by

$$\begin{aligned} q_u(t) = &(s_{u,I}(t-n\tau) + js_{u,Q}(t-n\tau))e^{j\phi_{u,u}(t)} \otimes \mathcal{A}_u(t) \otimes c_{u,u}(t-\tau_u) \\ &+ \sum_{m=0,\, m\neq u}^{M-1} (s_{m,I}(t-n\tau) + js_{m,Q}(t-n\tau))e^{j\phi_{u,m}(t)} \otimes \Upsilon_{u,m}(t) \otimes c_{u,m}(t-\tau_m). \end{aligned} \tag{13}$$

It is clear from (13) that $q_u(t)$ is equal to the wanted channel encoded QAM symbols, phase shifted by $\phi_{u,u}(t)$, convolved with the autocorrelation function of sequence u and convolved with

the wanted channel CIR, $c_{u,u}(t-\tau_u)$ plus an expression for the co-channel interference. From (13), the co-channel interference consists of the $M-1$ unwanted channel encoded QAM symbols, phase shifted and convolved with their respective cross correlation functions and respective channel CIR's.

It should be noted that the wanted channel phase shift, $\phi_{u,u}(t)$ will be slowly varying and may be tracked out using a decision directed phase tracker. The phase tracked signal $q_{u,*}(t)$ becomes

$$q_{u,*}(t) = (s_{u,I}(t-n\tau) + js_{u,Q}(t-n\tau)) \otimes \mathcal{A}_u(t) \otimes c_{u,u}(t-\tau_u) + \sum_{m=0,\, m\neq u}^{M-1} (s_{m,I}(t-n\tau) + js_{m,Q}(t-n\tau))e^{j(\phi_{u,m}(t)-\phi_{u,u}(t))} \otimes \Upsilon_{u,m}(t) \otimes c_{u,m}(t-\tau_m). \quad (14)$$

As described below the spreading sequences are designed such that over twice the duration of the CIR the autocorrelation functions, $\mathcal{A}_m(t)$, approximate a Dirac function so that $A_u(t) \otimes c_{u,u}(t-\tau_u) \simeq c_{u,u}(t-\tau_u)$. Consequently, after phase tracking the processed received signal becomes

$$q_{u,*}(t) \simeq (s_{u,I}(t-n\tau) + js_{u,Q}(t-n\tau)) \otimes c_{u,u}(t-\tau_u) + \sum_{m=0,\, m\neq u}^{M-1} (s_{m,I}(t-n\tau) + js_{m,Q}(t-n\tau))e^{j(\phi_{u,m}(t)-\phi_{u,u}(t))} \otimes \Upsilon_{u,m}(t) \otimes c_{u,m}(t-\tau_m). \quad (15)$$

The CIR, $c_{u,u}(t-\tau_u)$, may be estimated using the decision directed desired channel QAM symbols. It is then provided to the Rake receiver as shown in Fig. 1. For robustness, at the beginning of each frequency hop a short stream of pilot symbols may be used to estimate the CIR in the presence of noise. Typically no more than 10 pilot symbols are necessary at the beginning of each frequency hop along with the decision directed CIR updates to provide for sufficiently accurate estimates of the CIR. The pilot symbols are equal to constant 1's for the real and imaginary parts of the QAM symbols thereby enabling the CIR to be measured directly.

The Rake processor is adjusted such that its impulse response, $Y_k(t)$, is the complex conjugate of the time reversed measured CIR denoted by $\hat{c}_{u,u}(t-\tau_u)$. In this way it presents the matched filter to the channel response maximizing the peak *signal to noise ratio (SNR)* at its output. The Rake receiver will be discussed in the next section.

III. Polyphase spreading sequence design for undistorted channel state estimation

In this system each data symbol is modulated with a polyphase spreading sequence that is unique for every user. As the sequences are data modulated, it is the aperiodic autocorrelation and cross correlation functions of the sequences that are important and not the periodic correlation function properties [1]. Ideally, each user should employ a spreading sequence whose aperiodic autocorrelation function is an ideal Dirac function, but this is not achievable. For binary sequences, the best spreading sequences are the Barker sequences [8], but the maximum length is only 13 bits and more processing gain is required for accurate CIR estimation requiring longer sequences. By using polyphase sequences, complex chip sequences with each chip having a different phase and unity magnitude, generalized Barker sequences, as they are known, have been obtained with lengths up to 63 chips [13]. Several approaches have been used in the design of generalized Barker sequences [13], [18]. Brenner et al [18] used stochastic methods to determine generalized Barker sequences for lengths up to 45. Borwein et al [13] used a combination of calculus and stochastic methods to determine generalized Barker sequences for lengths up to 63. Frank [14] presented polyphase sequences of length equal to the square of a prime q with good aperiodic autocorrelation functions. Golomb and Scholtz [15] investigated generalized Barker sequences and presented six-phase Barker sequences of lengths up to 13 chips. In [17], 60-phase sequences satisfying the Barker condition up to length 18 were reported. Chirp type sequences have been published with single and multiple chirps [19], [20].

However, none of these sequences has an aperiodic autocorrelation function that is an ideal Dirac function and if used as a spreading sequence will produce a distorted measurement of the CIR. The approach that is used in this paper is to design the sequences so that the aperiodic autocorrelation function is zero for time offsets less than the delay spread of the channel, but allowed to be non-zero for time offsets greater than the delay spread of the channel.

The sequence design procedure of [13] is used, but the design goal is novel. The significance of our work is that the sequences designed allow essentially *inter symbol interference (ISI)* free channel sounding and estimation. The sequence design starts with a polyphase sequence that has an ideal periodic autocorrelation function. Small changes to the phase angles of the sequence are applied in a recurrent procedure, retaining each phase change that results in an improvement

to the aperiodic autocorrelation function. The starting point is a sequence from the Chu [16] family of periodic, polyphase sequences defined by the phase sequence expressed in terms of N_c phase sequence coefficients in units of radians, as

$$\theta^{chu}(t) = \sum_{n=0}^{N_c-1} \theta_n^{chu}(t - nT_c) = \frac{\pi(n+1)n}{N_c}(t - nT_c), \tag{16}$$

where N_c is even. The periodic Chu sequences have an ideal autocorrelation function with a peak value of N_c and zero elsewhere and the aperiodic autocorrelation function is not too bad.

In the sequence design procedure the recurrently modified aperiodic phase sequence is denoted as $\theta(t)$ and an iterated phase sequence is denoted as $\zeta(t)$. Initially $\theta(t)$ is set equal to $\theta^{chu}(t)$. The sequence $\zeta(t)$ is defined by

$$\zeta(t) = \sum_{n=0}^{N_c-1} \theta_n(t - nT_c) + a(n)\upsilon_c(t - nT_c), \tag{17}$$

where $a(n)$ is a random variable taking values 0, 1 and -1 and υ_c is a small constant phase angle. The sequence $\theta(t)$ is set equal to $\zeta(t)$ if the sum of the first β magnitudes of the aperiodic autocorrelation function of $\zeta(t)$ is less than that of $\theta(t)$. That is

$$\theta(t) = \zeta(t) \tag{18}$$

if and only if

$$\sum_{\tau=1}^{\beta} |\mathcal{A}_\theta(\tau)| - |\mathcal{A}_\zeta(\tau)| > 0, \tag{19}$$

where

$$\mathcal{A}_\theta(\tau) = \int_{-\infty}^{\infty} \sum_{n=0}^{N_c-1} e^{j\{\theta_n\}(nT_c)} \delta(t - nT_c) \sum_{n=0}^{N_c-1} e^{-j\{\theta_n\}(\tau + nT_c)} \delta(t - \tau - nT_c) dt. \tag{20}$$

Typically after less than 100 iterations of $\zeta(t)$ a converged result for $\theta(t)$ is obtained. An oversampled example[1] is shown in Fig. 2a, where the sequence length is 32 chips and β is 8 chips.

The aperiodic autocorrelation function of this sequence is shown in Fig. 3a. It can be seen that its sidelobes are zero for time offsets up to plus and minus 8 chips from the peak. Compared to a generalized Barker sequence, the sidelobe magnitude levels have increased, but the maximum value is only 2.2 compared to unity.

[1]Oversampling is used in Figures 2-7.

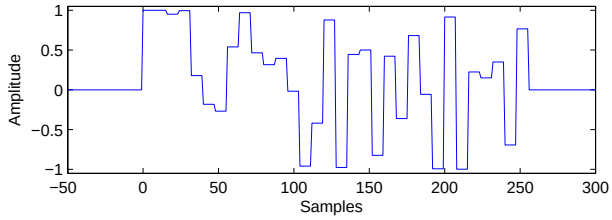

(a) Real part for user $m = 0$ sequence.

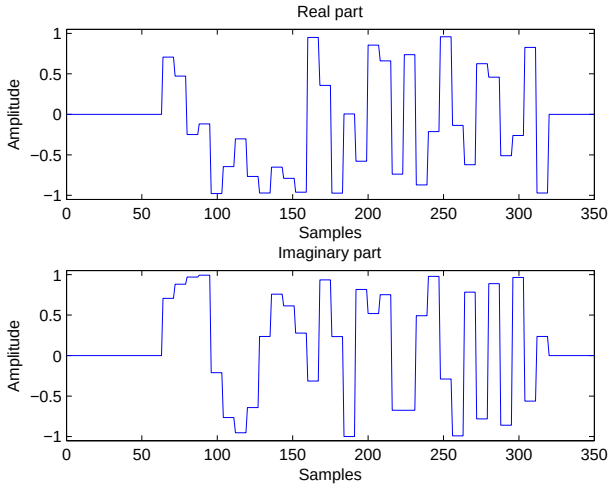

(b) Real and imaginary parts for user $m = 3$ sequence.

Fig. 2: Designed polyphase sequences of length 32 chips for users $m = 0$ and $m = 3$.

It has long been known that for polyphase sequences the autocorrelation function is invariant to any constant phase offset and/or any constant frequency offset. Accordingly, it is customary to apply a phase and frequency offset such that the first two values of the phase sequence are zero. From the above it follows that a family of polyphase sequences may be defined where each sequence has the same desired autocorrelation function. The sequences are defined for each user m, by

$$\theta(t) = \sum_{n=0}^{N_c-1} \left(\theta_n + \frac{2\pi mn}{N_c} \right) (t - nT_c). \tag{21}$$

With m constrained to be an integer, then m may range from $-\frac{N_c}{2}$ to $\frac{N_c}{2} - 1$. The relative phase

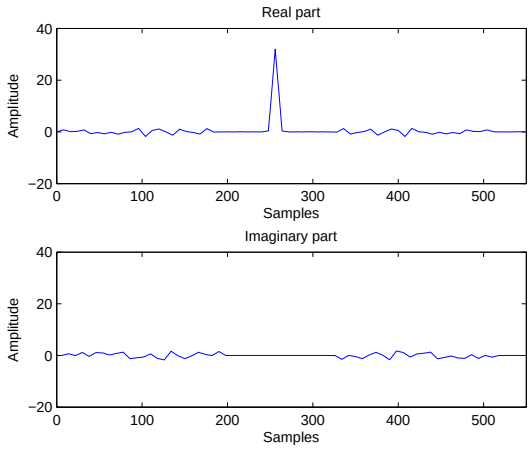

(a) Autocorrelation for $m = 0$ sequence.

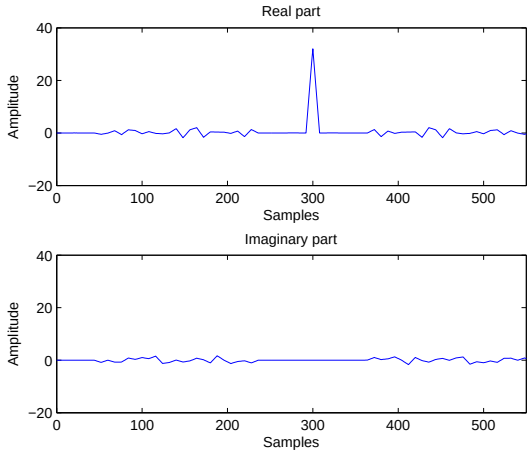

(b) Autocorrelation for $m = 3$ sequence.

Fig. 3: Autocorrelation functions of the designed polyphase sequence of length 32 chips (real and imaginary parts) for $m = 0$ and $m = 3$.

shift between any two sequences over the sequence length, is a multiple of 2π. For zero time offset the cross correlation is zero. It is apparent there are at most N_c different sequences.

A. Example: Polyphase sequences and Rake processing

We now give an example of the proposed polyphase sequences. The coefficients of $x_{m,I}(t)$ and $x_{m,Q}(t)$ in (5) can be defined in terms of the phase sequence for user m as

$$x_{m,I}(t) + jx_{m,Q}(t) = e^{j(\theta_n + \frac{2\pi mn}{N_c})}\delta(t - nT_c). \tag{22}$$

We define our example phase sequence of length 32, for $m = 0$, in (22) as

$$\begin{aligned}[\theta_0, \cdots, \theta_{31}] =& [0, 0, 25.7, 1.2, 79.7, 100.5, 106.1, 56.8, \\ & 346.3, 293.8, 288.4, 293.3, 94.2, 164.6, 245.2, 332.2, \\ & 170.3, 59.4, 60.0, 216.8, 295.0, 111.2, 46.0, 270.0, \\ & 172.1, 21.6, 184.9, 282.1, 81.9, 290.8, 134.5, 318.2]. \end{aligned} \tag{23}$$

In general the CIR will consist of a relatively large number of paths with index p and different complex attenuation factors $\alpha_{p,f}$, which depend upon the characteristics of the path. The CIR is defined as

$$\hat{c}(t) = \sum_{p=0}^{P-1} \alpha_{p,f}\, \delta(t - T_{p,f}), \tag{24}$$

where $T_{p,f}$ is the propagation delay of the path. As an example, consider that the net CIR including relative carrier phase shifts is

$$\hat{c}(t) = 0.25\delta(t + 2T) + j\delta(t) - 0.5\delta(t - 3T). \tag{25}$$

The real and imaginary parts of the output of the matched FIR filters in the receiver, $q(t)$, are shown in Fig. 4. It can be seen that the real part has a positive peak of 8, arising from the $0.25\delta(t + 2T)$ part of the CIR and has a negative peak of 16, arising from the $-0.5\delta(t - 3T)$ part of the CIR. The imaginary part has a positive peak of 32, arising from the $j\delta(t)$ part of the CIR.

By way of this example for the CIR, the procedure for programming the Rake processor follows standard usage. The measured time reversed CIR is

$$\hat{c}_o(t) = 8\delta(t + 2T) + j32\delta(t) - 16\delta(t - 3T). \tag{26}$$

The Rake processor is adjusted such that its impulse response, $Y_k(t)$, is the complex conjugate of the time reversed measured CIR $\hat{c}_o(t)$, giving

$$Y_k(t) = -16\delta(t + 3T) - j32\delta(t) + 8\delta(t - 2T). \tag{27}$$

In this way it presents the matched filter to the CIR maximizing the peak SNR at the Rake processor output. The peak signal output of the Rake processor, $P_{Rake}(t)$, for each data symbol

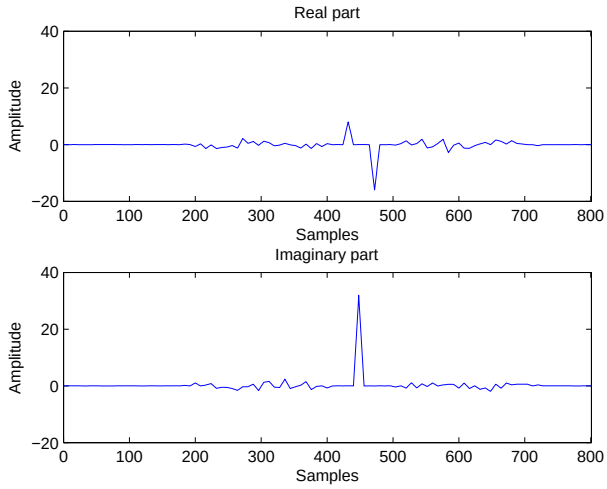

Fig. 4: Cross correlation of waveform of length 32 chips showing CIR (real and imaginary parts).

is given by

$$\begin{aligned} P_{Rake}(t) &= -16\delta(t+3T-nT_c) \times -16\delta(t-3T-nT_c) + j32\delta(t-nT_c) \times -j32\delta(t-nT_c) \\ &\quad + 8\delta(t-2T-nT_c) \times 8\delta(t+2T-nT_c)(s_I(t-nT_c) + js_Q(t-nT_c)) \\ &= (256+1024+64)\delta(t-nT_c)(s_I(t-nT_c) + js_Q(t-nT_c)) \\ &= 1344\delta(t-nT_c)(s_I(t-nT_c) + js_Q(t-nT_c)). \end{aligned} \tag{28}$$

The peak signal output has a value of 1344 due to Rake processing and the peak SNR is $\frac{1344^2}{N_w(64+1024+256)} = \frac{1344}{N_w}$, where N_w is the average noise power of each time sample. Without Rake processing the peak SNR which corresponds to the highest value radio path would only be $\frac{1024}{N_w}$. Consequently the Rake processing improves the peak SNR for this example by 1.2 dB.

B. Multiple Transceivers

When using multiple transceivers in a common frequency band the interference between users is reduced by the polyphase sequence design and by using frequency and time hopping. It is assumed that each receiver has acquired synchronization with its respective transmitter. It was stated above that if the sequences are offset in frequency the aperiodic autocorrelation functions are identical and the cross correlation interference may be reduced. This is formalized by the

following theorem:

Theorem 1:

The magnitude of the autocorrelation function, $A_{\hat{\theta}}(\tau)$, of a complex signal defined by the phase sequence

$$\hat{\theta}(t) = \sum_{n=0}^{N_c-1} \{\theta_n + n\psi\}(nT_c) \tag{29}$$

is equal to the magnitude of the autocorrelation function of a complex signal defined by the phase sequence

$$\theta(t) = \sum_{n=0}^{N_c-1} \theta_n(nT_c), \tag{30}$$

where ψ is a fixed phase value.

Proof:

$$A_{\hat{\theta}}(\tau) = \int_{-\infty}^{\infty} \sum_{n=0}^{N_c-1} e^{j\{\theta_n+n\psi\}(nT_c)}\delta(t-nT_c) \sum_{n=0}^{N_c-1} e^{-j\{\theta_n+n\psi\}(\tau+nT_c)}\delta(t-\tau-nT_c)dt. \tag{31}$$

$A_{\hat{\theta}}(\tau)$ is non-zero only when $\tau = \alpha T_c$, where α is an integer. Consequently

$$\begin{aligned}
A_{\hat{\theta}}(\alpha T_c) &= \int_{-\infty}^{\infty} \sum_{n=0}^{N_c-1} e^{j\{\theta_n+n\psi\}(nT_c)}\delta(t-nT_c) \sum_{n=0}^{N_c-1} e^{-j\{\theta_n+n\psi\}(\alpha T_c+nT_c)}\delta(t-\alpha T_c-nT_c)dt \\
&= \int_{-\infty}^{\infty} \sum_{n=0}^{N_c-1-\alpha} e^{j\{\theta_{n+\alpha}+n\psi+\alpha\psi\}(nT_c)} e^{-j\{\theta_n+n\psi\}(nT_c)}\delta(t-nT_c)dt \\
&= e^{j\alpha\psi} \int_{-\infty}^{\infty} \sum_{n=0}^{N_c-1-\alpha} e^{j\{\theta_{n+\alpha}-\theta_n\}(nT_c)}\delta(t-nT_c)dt \qquad (32) \\
&= e^{j\alpha\psi} A_{\theta}(\alpha T_c) \qquad (33)
\end{aligned}$$

and so

$$|A_{\hat{\theta}}(\tau)| \;=\; |A_{\theta}(\tau)|. \tag{34}$$

By making $N_c m\psi$ an integral multiple of 2π for each user m, the cross correlation between sequences for different users and zero time offset will be zero. This can be seen by considering transmitting user m and receiver user u. For zero time offset the cross correlation, $C_{\hat{\theta}}(0)$, is

given by

$$C_{\hat{\theta}}(0) = \int_{-\infty}^{\infty} \sum_{n=0}^{N_c-1} e^{j\{\theta_n+nm\psi\}(nT_c)}\delta(t-nT_c) \sum_{n=0}^{N_c-1} e^{-j\{\theta_n+un\psi\}(nT_c)}\delta(t-nT_c)dt$$
$$= \int_{-\infty}^{\infty} \sum_{n=0}^{N_c-1} e^{j\{\theta_n+mn\psi\}(nT_c)}e^{-j\{\theta_n+un\psi\}(nT_c)}\delta(t-nT_c)dt$$
$$= \int_{-\infty}^{\infty} \sum_{n=0}^{N_c-1} e^{jn\psi(m-u)(nT_c)}\delta(t-nT_c)dt$$
$$= 0. \tag{35}$$

Accordingly with the sequence of phases for the polyphase sequence designed for ideal autocorrelation function, expressed here in radians, as θ_i for $i = 0$ to $N_c - 1$, the real and imaginary sequences for the transmitter of user m, defined by $x_{m,I}(t)$ and $x_{m,Q}(t)$, are given by

$$x_{m,I}(t) = \sum_{n=0}^{N_c-1} \Big\{cos(\theta_n(nT_c))cos\Big(\frac{2\pi nm}{nT_c}\Big) - sin(\theta_n(nT_c))sin\Big(\frac{2\pi nm}{nT_c}\Big)\Big\}\delta(t-nT_c) \tag{36}$$

and

$$x_{m,Q}(t) = \sum_{n=0}^{N_c-1} \Big\{sin(\theta_n(nT_c))cos\Big(\frac{2\pi nm}{nT_c}\Big) + cos(\theta_n)sin\Big(\frac{2\pi nm}{nT_c}\Big)\Big\}\delta(t-nT_c). \tag{37}$$

Up to N_c different waveforms are defined by (36) and (37) for $m = 0$ to $N_c - 1$ corresponding to up to N_c users each transmitting different spreading sequences. For non-zero time offsets the cross correlation between sequences is not zero. However, the total level of interference experienced at each receiver is mitigated by the frequency and time hopping, averaged over the number of multipaths and by forward error correction using soft decision decoding.

For example, Fig. 2b shows the user $m = 3$ plots of the real, $x_{3,I}(nT_c)$, $n = 0, \cdots, N_c - 1$, and imaginary sequences, $x_{3,Q}(nT_c)$, $n = 0, \cdots, N_c - 1$. In comparison, the real sequence for the transmitter, $m = 0$ was shown in Fig. 2a. The real and imaginary parts of the autocorrelation function for the sequences obtained with $m = 3$ are shown in Fig. 3b. It will be noticed from Fig. 3b that the real part has a zero response surrounding the main peak amplitude of 32, for 8 chips on either side of the main peak as was obtained before, for $m = 0$ in Fig. 3a. However, it can be noted that the sidelobes in Fig. 3b are not the same as those in Fig. 3a. Similarly, the imaginary part shown in Fig. 3b, for $m = 3$, is similar to that in Fig. 3a for $m = 0$, and also has a zero response over the central corresponding interval of 16 chip periods.

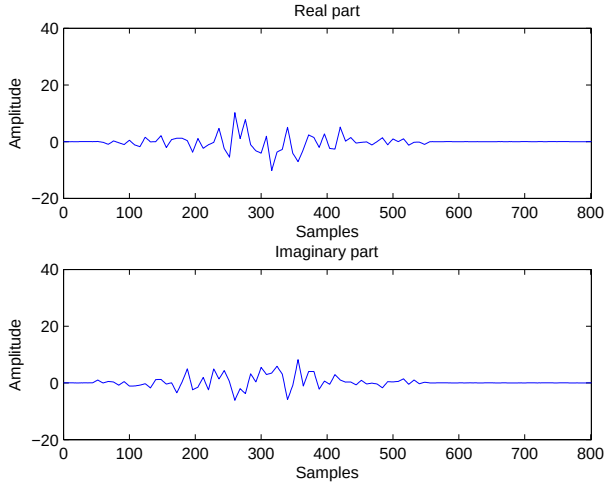

Fig. 5: Cross correlation of waveforms of length 32 chips (real and imaginary parts), $m = 0$ and $m = 3$.

The level of interference experienced by the receiver for $m = 0$, when the transmitter for $m = 3$ is transmitting (or vice versa) is shown in Fig. 5 for the real and imaginary parts. The worst case interference level is -10.2 for the real part and 8.2 for the imaginary part, but these do not occur at the same time. In practice, the interference values will be a function of the hopping centre frequencies, time hopping, the CIRs (the channel impulse from the transmitter causing interference will be different from the channel impulse from the transmitter of the wanted signal) and the residual timing/ phase of the desired signal correlation. Time hopping is employed in which each transmitted waveform is subject to a pseudo random timing offset controlled by a pseudo random number generator in each transmitter and plays a key role in averaging the effects of interference. A training sequence may be used to enable the receiver to synchronize an identical pseudo-random generator [1]. Powerful forward error correction coding is also used and we provide examples using a Low Density Parity Check (LDPC) code, specifically one of the WiMax codes [12] and soft decision, iterative decoding [11] which produces good performance in this application.

IV. Evaluation of the Communication Channel

The communication channel consists of multiple, non line of sight paths from multiple transmitters located within a building or adjacent buildings. In a typical application, transmitters will be located in fixed locations, but some may be mobile. Variations in multipath conditions will depend upon movement, mostly people moving in the building and can be expected to be slowly varying relative to the duration of radio transmission formatted in frames or packets. A widely accepted statistical distribution for these circumstances is log normal fading for each path and a comprehensive survey of the literature supporting this model for indoor radio transmission was presented by Hashemi [21].

At the receiver, the wanted signal is summed, voltage wise, in the Rake processor with the received power in each path log normally distributed with attenuation factor $\alpha_{p,f}$ and a total number of P paths. The total interference level in the receiver depends upon the attenuation levels of each path $\beta_{m,q,f}$, from each of the interfering transmitters relative to the wanted signal receiver and the cross correlation values between the respective polyphase sequences. The number of different paths from each transmitter to the receiver need not be the same, but for simplicity we have assumed they are equal to Q. Time hopping is employed in order to cause a variation in these correlation values as well as to cause a change in the relative carrier phase shifts. Frequency hopping is used to change the path attenuations for the wanted signal and to reduce the interference from other users. It is expected that a typical system will use a total number, N_F of between 3 and 10 non-overlapping channels. Frequency hopping may employ any number of discrete hopping centre frequencies, uniformly distributed across the allocated spectrum. In the analysis below we have restricted the hopping frequencies to the centre frequencies of each contiguous channel.

The analysis of the complete communications channel is quite involved and the probability distributions for the *signal to interference and noise ratio (SINR)* and associated outage probabilities are derived in detail in the Appendix.

V. Simulation Results

Forward error correction coding is employed in the form of the WiMax (1056, 528) LDPC code [12] and iterative decoding (100 iterations per received vector) and the baseline *frame error rate (FER)* performance is shown in Fig. 6a. It is plotted against $\frac{E_b}{N_0}$ in dB, where E_b is the

energy per information bit and N_0 is the noise power spectral density. The frame error rate is used instead of the bit error rate or symbol error rate due to the use of block coding. It is shown in [23] that this is the key performance parameter for block coded systems using codes such as turbo codes and LDPC codes. These results were obtained by simulation using the 32 chip waveforms defined in (36) and (37) with the phase values given in (23). In deriving Fig. 6a, Rake processing for 17 paths was assumed, but the processing gain is normalized out by plotting against $\frac{E_b}{N_0}$. For M users, all M transmitters are assumed to be transmitting with equal power. In Fig. 6a there is no frequency hopping and all of the M users occupy a single, common channel. The importance of frequency hopping is indicated by the corresponding baseline performance improvement shown in Fig. 6b when there are $N_f = 5$ hopping channels. It can be seen that for 20 users operating at a FER of 10^{-4}, $\frac{E_b}{N_0} = 2.95dB$ is sufficient when frequency hopping is deployed, but that 8.8dB is required when there is no frequency hopping.

The baseline performance shown in Fig. 6 does not take into account the statistical variation of the received SINR which is analysed in the Appendix. The received, wanted signal power varies with the channel path attenuation factors, $\alpha_{p,f}$, and these determine the received SNR, E_S/N_0, and the path attenuation factors, $\beta_{m,q,f}$, for the (M-1) interfering transmitters. This coupled with carrier phase shifts and cross correlation coefficients between respective sequences determine the total interference power.

The distribution of the wanted signal power can be obtained by simulation and is shown in Fig. 7a for $P = 17$ wanted user paths. The average of this distribution is 14.86 dB corresponding to a multipath gain. The variance is 1.67 dB.

The distribution of the SINR is shown in Fig. 7b for $M = 25$, single path $E_S/N_0 = 5$ dB. The multipath E_S/N_0 includes the gain due to the Rake receiver. This gain was measured by simulation and can be accurately calculated using (61) from the appendix. For $P = 17$ it is 14.86 dB. It will be noticed that there is a considerable reduction in the variance of the SINR distribution. These results are consistent with those obtained by other researchers [27].

We are interested in the number of users that the system can support for a given number of paths and a given value of transmitter power, defined by E_S/N_0. For this, we can plot SINR$_x$ curves given by

$$P\{\text{SINR} < \text{SINR}_x\} = P_x. \tag{38}$$

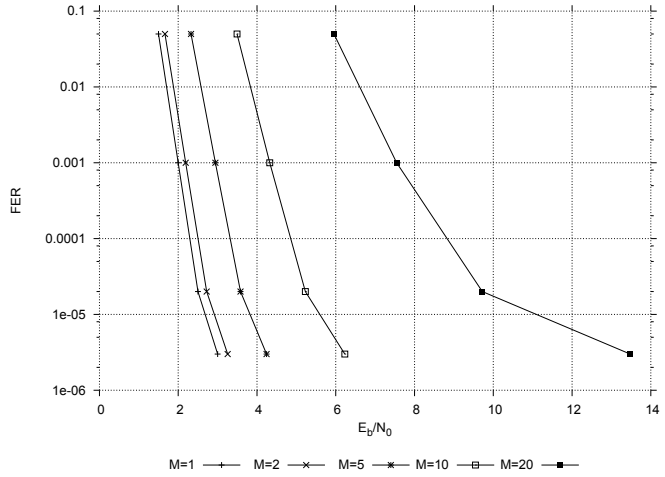

(a) FER with no frequency hopping.

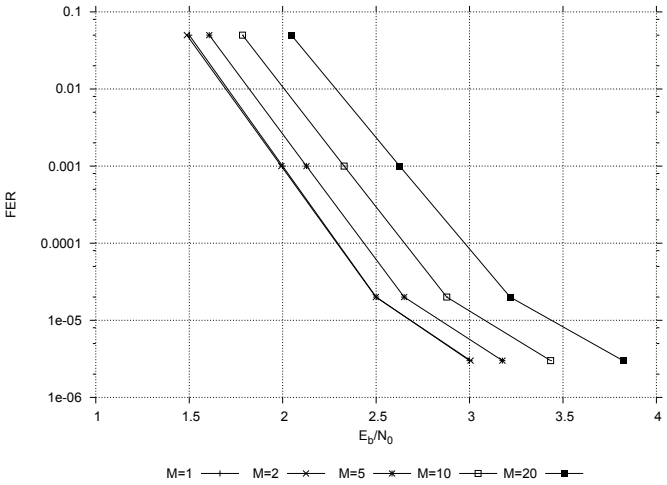

(b) FER using frequency hopping over 5 channels.

Fig. 6: FER using the WiMax(1056,528) LDPC code and M simultaneous transmitters.

This can be estimated from simulation by obtaining and analysing SINR histograms such as the example shown in Fig. 7b. The estimate of P_x is the tail area of the histogram for values of SINR $<$ SINR$_x$.

The required SINR$_x$ is determined from an acceptable value for P_x, the outage probability. The outage is due to the combined effects of wanted signal propagation, other user interference propagation and AWGN. The intersection of the SINR$_x$ curves with the SINR necessary for acceptable performance from the LDPC decoder (FEC SINR) defines an operating point for the

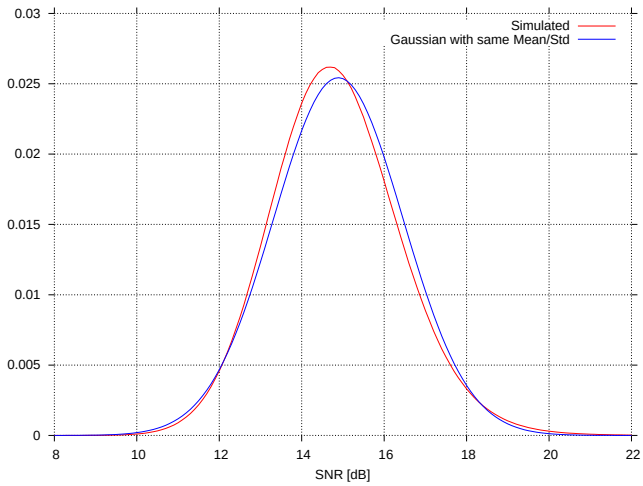

(a) Single user post Rake SNR distribution for single path $E_S/N_0 = 0$ dB and $P = 17$ (mean 14.86 dB, variance 1.67 dB).

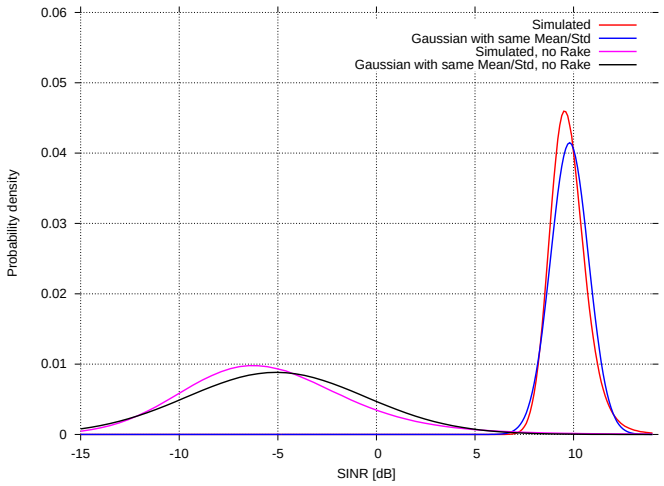

(b) Multiuser post Rake SINR distribution for single path $E_S/N_0 = 5$ dB, $P = 17$ and $M = 25$ users. The curves on the left are for no Rake, while those on the right employ the Rake processor.

Fig. 7: Post Rake distributions.

system and determines how many users can be accommodated at a given E_S/N_0. If the SINR$_x$ is lower than the FEC SINR, then the LDPC decoder will produce an unacceptable number of bits in error.

The histograms were produced for a large number of E_S/N_0 values and all values of M to obtain a 3D curve (SINR$_x$ against M and E_S/N_0). We can also plot the intersection between this curve and the plane at the FEC SINR level. These intersections are 2D plots showing the

compromise between M and E_S/N_0 at the limit SINR of the error correction. Any point to the left of these plots is an achievable point with outage probability less than P_x. The 3D and 2D plots are shown against different values P_x in Fig. 8a and different values of N_F in Fig. 8b.

In Fig. 8a we can see the influence of the value of required P_x on the system. For example, for $P_x = 10^{-5}$ and $E_S/N_0 = 0$ dB the system can accommodate up to 13 users. If we wanted 15 users, the E_S/N_0 cannot be lower than approximately 2 dB. However, if the required $P_x = 10^{-4}$ then for $E_S/N_0 = 0$ dB up to 17 users can be accommodated.

In Fig. 8b we can see the influence of the number of contiguous hopping channels on the system for $P_x = 10^{-3}$ and $P = 17$. With a single channel there cannot be more than about 6 users, no matter how much transmitter power is used (the graph is asymptotic in E_S/N_0). This value increases to 12 users for $N_F = 2$ channels and up to 28 users for $N_F = 5$. With $E_S/N_0 = 0$ dB, the values become $M = 4, 8, 13, 18, 23$ for $N_F = 1, 2, 3, 4, 5$, respectively.

VI. Conclusions

In this paper we have introduced novel polyphase spreading sequences which each have the same idealized autocorrelation function having near zero value (of length exceeding the delay spread of the channel) on each side of the autocorrelation peak. This feature allows the multipath channel impulse response to be measured accurately in order to optimize the processing gain of a Rake receiver. By offsetting a polyphase sequence in frequency, it was proven that a single sequence design can be used to produce a family of sequences, each having the same autocorrelation function. It was also shown that low levels of autocorrelation sidelobes lead to low levels of cross correlation between sequences and low levels of mutual interference between users.

With multiple paths between users and log-normal slow fading combined with frequency and time hopping, exact analysis of SINRs is quite involved. A model giving statistics for the SINR as a function of the number of users was presented which provides a useful indication of expected performance.

Simulation results were presented that show that in practical applications, a relatively large number of simultaneous users can be supported without the need for excessive increases in transmitter power compared to that necessary for a single user.

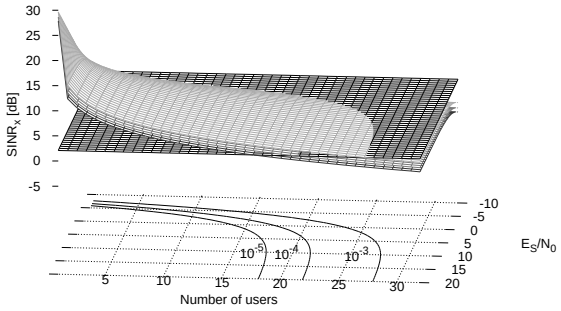

(a) For parameter P_x ($P = 17$, $N_F = 5$).

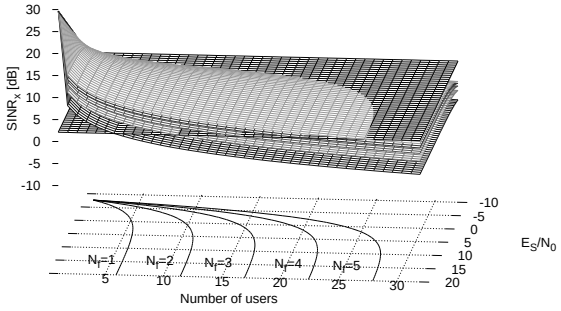

(b) For parameter N_F ($P = 17$, $P_x = 10^{-3}$).

Fig. 8: SINR$_x$ [dB] graphs.

VII. Appendix

The signal power, P_A, interference power (from other users), P_I, and noise power (after the matched filter), P_N, can be expressed as

$$P_A = \frac{1}{N_F} \sum_{f=0}^{N_F-1} \left(\sum_{p=0}^{P-1} \alpha_{p,f}^2 \right)^2 \tag{39}$$

$$P_I = \overline{|\Upsilon|^2} \frac{1}{N_F^2} \sum_{f=0}^{N_F-1} \left(\sum_{p=0}^{P-1} \alpha_{p,f}^2 \right) \left(\sum_{m=1}^{M-1} \sum_{q=0}^{Q-1} \beta_{m,q,f}^2 \right) \tag{40}$$

$$P_N = \sigma^2 \frac{1}{N_F} \sum_{f=0}^{N_F-1} \left(\sum_{p=0}^{P-1} \alpha_{p,f}^2 \right) \tag{41}$$

$$\sigma^2 = \frac{1}{2RE_S/N_0}, \tag{42}$$

where $R = 1/2$ is the rate of the error correction code and $\overline{|\Upsilon|^2}$ is the average squared absolute cross-correlation value between the wanted user and other users. The averaging is across all paths and all users and also all time hopping offsets.

The path attenuation factors are log-normally distributed and are changing slowly relative to the data rate. This means that they are almost constant for a large number of LDPC blocks. The log-normal distribution has a large variance, which in turn means that for the same parameters (e.g. P, M, N_F) we can have quite a large variance in the values of SINR over time, where we can write

$$\text{SINR} = 10 \log_{10} \frac{P_A}{P_I + P_N}. \tag{43}$$

$$\text{SINR} = 10 \log_{10} N_F + 10 \log_{10} \frac{\sum_{f=0}^{N_F-1} \left(\sum_{p=0}^{P-1} \alpha_{p,f}^2 \right)}{\overline{|\Upsilon|^2} \sum_{f=0}^{N_F-1} \left(\sum_{p=0}^{P-1} \alpha_{p,f}^2 \right) \left(\sum_{m=1}^{M-1} \sum_{q=0}^{Q-1} \beta_{m,q,f}^2 \right) + \sigma^2 N_F \sum_{f=0}^{N_F-1} \left(\sum_{p=0}^{P-1} \alpha_{p,f}^2 \right)} \tag{44}$$

For analysis of how often the SINR is within a given range, it may be assumed the SINR values have a Gaussian distribution and determine the mean $E\,(\text{SINR})$ and standard deviation $Std\,(\text{SINR})$. However, the actual shape of the distribution and also the mean and standard deviation depend on the number of propagation paths and these have been derived by simulation and compared to the analysis.

Using (39), (40) and (41) we can write the SINR as in (44). We denote

$$A_f = \sum_{p=0}^{P-1} \alpha_{p,f}^2 \tag{46}$$

$$I_f = \sum_{q=0}^{Q-1} \sum_{m=1}^{M-1} \beta_{m,q,f}^2. \tag{47}$$

Then we can write

$$\text{SINR} = 10 \log_{10} N_F + 10 \log_{10} \frac{\sum_{f=0}^{N_F-1} A_f^2}{\sum_{f=0}^{N_F-1} A_f (\overline{|\Upsilon|^2} I_f + \sigma^2 N_F)}. \tag{48}$$

For a single channel we have

$$\begin{aligned}\text{SINR} &= 10\log_{10} N_F + 10\log_{10}\frac{A_f^2}{A(\overline{|\Upsilon|^2}I_f + \sigma^2 N_F)} \\ &= 10\log_{10} N_F + 10\log_{10}\frac{A_f}{\overline{|\Upsilon|^2}I_f + \sigma^2 N_F} \\ &= 10\log_{10} N_F + 10\log_{10} A_f - 10\log_{10}(\overline{|\Upsilon|^2}I_f + \sigma^2 N_F). \end{aligned} \quad (49)$$

Noting that the two random variable terms are statistically independent we have

$$E(\text{SINR}) = 10\log_{10} N_F + E(10\log_{10} A_f) - E\left(10\log_{10}(\overline{|\Upsilon|^2}I_f + \sigma^2 N_F)\right) \quad (50)$$

$$Var(\text{SINR}) = Var(10\log_{10} A_f) - Var\left(10\log_{10}(\overline{|\Upsilon|^2}I_f + \sigma^2 N_F)\right). \quad (51)$$

We use the log-normal approximation discussed in [24] in deriving the mean and variance of a sum of log-normal variables. It also has the advantage of a closed solution which will allow us to evaluate the influence of each parameter. The approximation to a sum of log-normally distributed random variables, X, is

$$Var(\log X) = \log\left(1 + \frac{Var(X)}{E(X)^2}\right) \quad (52)$$

$$E(\log X) = \log E(X) - \frac{1}{2}Var(\log(X)) \quad (53)$$

Denote $\mu = E(\alpha^2) = 1.94$. To use the log-normal approximation in [24] for A_f and $\overline{|\Upsilon|^2}I_f + \sigma^2 N_F$ we need

$$E(A_f) = E\left(\sum_{p=0}^{P-1}\alpha_{p,f}^2\right) = P\mu \quad (54)$$

$$Var(A_f) = Var\left(\sum_{p=0}^{P-1}\alpha_{p,f}^2\right) = PVar\left(\alpha_{p,f}^2\right) = P\mu^2(\mu^2 - 1) \quad (55)$$

$$\begin{aligned} E\left(\overline{|\Upsilon|^2}I_f + \sigma^2 N_F\right) &= E\left(\overline{|\Upsilon|^2}\sum_{q=0}^{Q-1}\sum_{m=1}^{M-1}\beta_{m,q,f}^2 + \sigma^2 N_F\right) \\ &= \overline{|\Upsilon|^2}(M-1)Q\mu + \sigma^2 N_F \end{aligned} \quad (56)$$

$$\begin{aligned} Var\left(\overline{|\Upsilon|^2}I_f + \sigma^2 N_F\right) &= Var\left(\overline{|\Upsilon|^2}\sum_{q=0}^{Q-1}\sum_{m=1}^{M-1}\beta_{m,q,f}^2 + \sigma^2 N_F\right) \\ &= \overline{|\Upsilon|^2}^2(M-1)Q\mu^2(\mu^2-1). \end{aligned} \quad (57)$$

For notation conciseness, denote

$$\lambda = 1 + \sigma^2 N_F / \overline{|\Upsilon|^2}(M-1)Q\mu \geq 1 \tag{58}$$

Then, if $A_f, I_f\overline{|\Upsilon|^2} + \sigma^2 N_F$ are approximately log-normal, their logs are normal and we can calculate their mean and variance as

$$Var\left(\log A_f\right) = \log\left(1 + \frac{Var\left(A_f\right)}{E\left(A_f\right)^2}\right) \qquad = \log\left(1 + \frac{\mu^2 - 1}{P}\right) \tag{59}$$

$$\begin{aligned} Var\left(\log(\overline{|\Upsilon|^2} I_f + \sigma^2 N_F)\right) &= \log\left(1 + \frac{Var\left(\overline{|\Upsilon|^2} I_f + \sigma^2 N_F\right)}{E\left(\overline{|\Upsilon|^2} I_f + \sigma^2 N_F\right)^2}\right) \\ &= \log\left(1 + \frac{\mu^2 - 1}{(M-1)Q\lambda^2}\right) \end{aligned} \tag{60}$$

$$\begin{aligned} E\left(\log A_f\right) &= \log E\left(A_f\right) - \frac{1}{2} Var\left(\log\left(A_f\right)\right) \\ &= \log P\mu - \frac{1}{2}\log\left(1 + \frac{\mu^2 - 1}{P}\right) \end{aligned} \tag{61}$$

$$\begin{aligned} E\left(\log(\overline{|\Upsilon|^2} I_f + \sigma^2 N_F)\right) &= \log E\left(\overline{|\Upsilon|^2} I_f + \sigma^2 N_F\right) - \frac{1}{2} Var\left(\log\left(\overline{|\Upsilon|^2} I_f + \sigma^2 N_F\right)\right) \\ &= \log \overline{|\Upsilon|^2}(M-1)Q\mu\lambda - \frac{1}{2}\log\left(1 + \frac{\mu^2 - 1}{(M-1)Q\lambda^2}\right) \end{aligned} \tag{62}$$

$$\begin{aligned} E\left(\text{SINR}\right) &= 10\log_{10} N_F + \left(\frac{10}{\log 10}\right)\left(E\left(\log A_f\right) - E\left(\log(\overline{|\Upsilon|^2} I_f + \sigma^2 N_F)\right)\right) \\ &= 10\log_{10}\left(\frac{N_F}{(M-1)\lambda\overline{|\Upsilon|^2}}\frac{P}{Q}\right) + 5\log_{10}\frac{1 + \frac{\mu^2-1}{(M-1)Q\lambda^2}}{1 + \frac{\mu^2-1}{P}} \end{aligned} \tag{63}$$

$$E\left(\text{SINR}\right) \rightarrow \qquad 10\log_{10}\left(\frac{N_F}{(M-1)\lambda\overline{|\Upsilon|^2}}\frac{P}{Q}\right) \text{ as } P, Q \rightarrow \infty \tag{64}$$

$$\begin{aligned} Var\left(\text{SINR}\right) &= \left(\frac{10}{\log 10}\right)^2 \left(Var\left(\log A_f\right) + Var\left(\log(\overline{|\Upsilon|^2} I_f + \sigma^2 N_F)\right)\right) \\ &= \left(\frac{10}{\log 10}\right)^2 \log\left(1 + \frac{\mu^2 - 1}{P}\right)\left(1 + \frac{\mu^2 - 1}{(M-1)Q\lambda^2}\right) \end{aligned} \tag{65}$$

$$Std\left(\text{SINR}\right) = \left(\frac{10}{\log 10}\right)\sqrt{\log\left(1+\frac{\mu^2-1}{P}\right)\left(1+\frac{\mu^2-1}{(M-1)Q\lambda^2}\right)} \tag{66}$$

$$Std\left(\text{SINR}\right) \to 0 \textbf{ as } P, Q \to \infty. \tag{67}$$

We note that $Std\left(\text{SINR}\right)$ decreases weakly and asymptotically with $\lambda \geq 1$ which is useful for analysis: the largest variability of SINR is in the absence of Gaussian noise ($\lambda = 1$).

From (64) it can be seen that the number of paths P has only an asymptotic effect on the mean of the SINR with respect to interference from other users. However the number of paths does affect the SNR through the Rake receiver gain. This can be seen in the noise term in (58). A greater number of paths results in a smaller standard deviation for SINR (67), which leads to a reduced outage probability for a given SNR.

REFERENCES

[1] Proakis, J.G.: 'Digital Communications'(McGraw-Hill, 1997)

[2] Saleh, A., Valenzuela, R.: 'A Statistical Model for Indoor Multipath Propagation', IEEE JSAC,1987, 5 (2), pp. 128-137

[3] Foerster, J., Li, Q.: 'UWB Channel Modeling Contribution from Intel', IEEE P802.15-02/279r0-SG3a, IEEE P802.15 Working Group for Wireless Personal Area Networks (WPANs), 2002

[4] Atarius et al.: 'Method and apparatus for configuring a RAKE receiver', US Patent 7382821, 2007

[5] Win, M.Z.,Scholtz, R.A.: 'Impulse radio: how it works', IEEE Commun. Letters,1998, 2 (2), pp.36 - 38

[6] Gold, R.,: 'Optimal binary sequences for spread spectrum multiplexing' (Corresp.), IEEE Trans. Inform. Theory,1967, 13 (4), pp. 619-621

[7] Kasami, T.: 'Weight Distribution Formula for Some Class of Cyclic Codes', 1966,Tech. Report No. R-285, Univ. of Illinois

[8] Barker, R.H.: 'Group synchronizing of binary digital systems', Communication Theory (W. Jackson, ed.) (Academic Press New York), 1953, pp. 273-287

[9] Gabor, D.: 'Theory of Communication', J.IEE, 1946, 93, pp. 429-457

[10] Couch, L.W.: 'Digital and Analog Communication Systems', (5^{th} ed. Prentice Hall), 1997

[11] Lin, S., Costello, D.J.: 'Error Control Coding' (2^{nd} ed. Pearson Prentice Hall), 2004

[12] WiMax Standard: 'IEEE Standard for Local and metropolitan area networks, Part 16: Air Interface for Fixed and Mobile Broadband Wireless Access Systems', 2005

[13] Borwein, P., Ferguson,R.: 'Polyphase sequences with low autocorrelation', IEEE Trans. Inform. Theory, 2005, 51 (4), pp. 1564-1567

[14] Frank, R.L.: 'Polyphase codes with good nonperiodic correlation properties', IEEE Trans. Inform. Theory, 1963, 9, pp. 43-45

[15] Golomb, S.W., Scholtz, R.A.: 'Generalized Barker sequences', IEEE Transactions on Information Theory,1965, 11 (4), pp. 533-537

[16] Chu, D.C.: 'Polyphase codes with good periodic correlation properties', IEEE Trans. Inform. Theory, 1972, 1, pp. 531-533

[17] Zhang, N., Golomb, S.W.: 'Sixty phase generalized Barker sequences', IEEE Trans. Inform. Theory, 1989, 35 (4), pp. 911-912

[18] Brenner, A.R.: ‘Polyphase Barker sequences up to length 45 with small alphabets’,IEE Electronic Letters, 1998, 34 (16), pp. 1576-1577

[19] Popovic, B.M.: ‘GCL polyphase sequences with minimum alphabets’,IEE Electronic Letters, 1994, 30, pp. 106-107

[20] Wysocki, B.J., Wysocki, T.A., Zepernick, H.J.: ‘Walsh-Chirp sequences for wireless applications’, Jnl Telecomms and Information Technology,2001, 2 (3), pp. 24-28

[21] Hashemi, H.: ‘The Indoor Radio Propagation channel’, Proc. IEEE, 1993, 81 (7), pp. 943-967

[22] Farazian, M., Gudem, P. S., Larson, L. E.: ‘Fast hopping frequency generation in digital CMOS’ (Springer 2013)

[23] Dolinar, S., Divsalar, D., Pollara, F.: ‘Code performance as a function of block size’ (TMO Progress report 42-133, 1998)

[24] Fenton, L.: ‘The sum of log-normal probability distributions in scatter transmission systems’, IRE Transactions on Communications Systems, 1960, 8 (1), pp. 57-67

[25] Tomlinson, M., Ambroze, M.A., Martin, P.A., Taylor, D.P.: ‘Broadband Wireless Communication System’, British Patent GB2476930, 2011

[26] Molisch, A. F., Foerster, J. R., Pendergrass, M.: ‘Channel models for ultra wideband personal area networks’, IEEE Transactions on Wireless Communication, 2003, 10 (6), pp. 14-21

[27] Arslan (Editor), H., Ning Chen (Editor), Z., Di Benedetto (Editor), M.: ‘Ultra Wideband Wireless Communication’ (Wiley 2006)